

## THE $^{13}\text{CO}$ DISTRIBUTION AND CORRELATION WITH EXTINCTION IN L134

MINN, YOUNG KEY AND LEE, HYE KYUNG

Department of Astronomy and Space Science  
Kyung Hee University, Yong-in, Kyonggi-do, 449-701 Korea  
(Received Mar. 7, 1996; Accepted Mar. 15, 1996)

### ABSTRACT

We mapped the  $^{13}\text{CO}$  line in the dark nebula L134 using the 14-m Taeduck radio telescope with a 57 arcsec beam and one beam spacing. The cloud has a spherical shape with an intensity peak ridge extended from the northwest to the southeast directions. The halfwidth and the radial velocity of the lines peak at the region of the cloud center. The radial velocity decreases from the cloud center towards the north and south directions. The integrated line intensity distributions in the space-velocity plane show some structure and a velocity gradient. The  $^{13}\text{CO}$  and  $\text{H}_2\text{CO}$  clouds and dark clouds are closely related in space in shape, outer boundary, and intensity peak positions. The  $^{13}\text{CO}$  integrated line intensity is linearly proportional to the visual extinction.

*Key Words* : galaxies: clustering—galaxies: intergalactic medium

### I. INTRODUCTION

L134 is a small and very opaque dark cloud located off the galactic plane at a distance of about 150pc. It has an angular diameter of about 40 arcmin corresponding to a linear diameter of 1.7pc. The minimum extinction in the core of the cloud in blue is  $A_B = 9.7$  magnitudes. Several molecules have been mapped in L134 by many authors ( $\text{H}_2\text{CO}$  by Sume et al.1975, Brooks et al.1976, and Downes et al.1976, CO by Mahoney et al.1976, Tucker et al.1976, and Martin and Barrett 1978, and OH by Mattila et al.1979). In addition, the molecular lines of CH, CS, HCN,  $\text{HCO}^+$ , HNC,  $\text{NH}_3$ , DNC, and  $\text{DCO}^+$  have been observed in one or a few positions in this cloud. We selected this cloud to map in the  $^{13}\text{CO}$  line to study the structure and kinematics of the cloud, and to compare the distribution of the molecule with that of dust. Since this cloud is an isolated object at high galactic latitude ( $l = 0^\circ$ ,  $b = 36^\circ$ ), we thought this cloud to be appropriate for the study of the structure of dark clouds, kinematics of the interstellar molecules in dark clouds, and the correlation between molecules and dust. L134 also has no associated energy source such as HII regions and young stars, and has a proper size for mapping with the 1 arcmin beam which is the main beam size of the telescope employed for this study. There are a few published CO maps of this cloud made previously by several authors, but the angular resolution of the maps is rather too poor to investigate the structure and kinematics of the cloud in detail. In this paper, we present the maps of distribution and kinematics of  $^{13}\text{CO}$  in L134 made with an arcmin beam and one beam spacing. We examined the structure and kinematics of the  $^{13}\text{CO}$  cloud and compared them with the structure of the apparent dark cloud and with the distribution of other molecules. We also examined the correlation between  $^{13}\text{CO}$  and dust.

### II. OBSERVATIONS

Observations were made with the 14-m Taeduck radio telescope through the year 1993. The half-power beamwidth is about 57 arcsec at the rest frequency of  $^{13}\text{CO}(J = 1 - 0)$ , 110.201353 GHz, and the beam efficiency  $\eta = 0.45$ . The receiver front end is a cooled 80-120 GHz Schottky diode mixer. The system temperature, measured with room-temperature was typically 800-1000K. The backend is a 256 channel filter bank having 250 kHz bandwidth

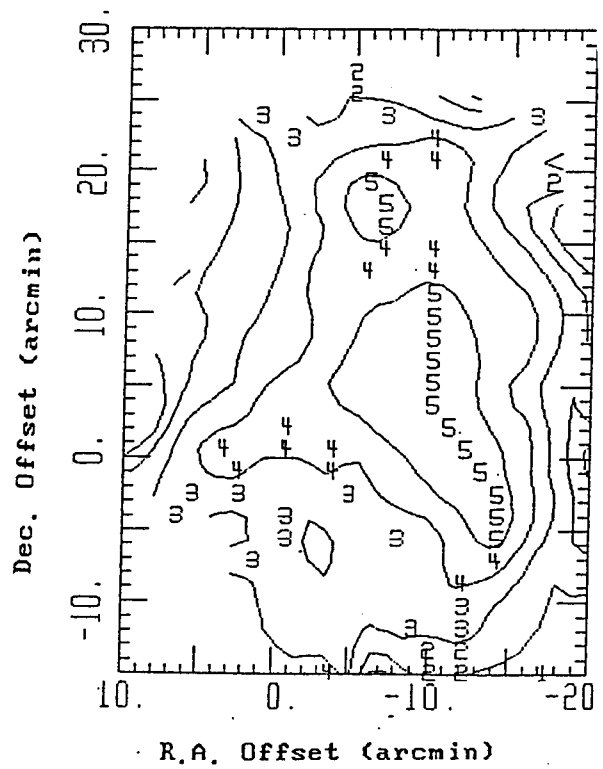


Fig. 1. Contour map of  $^{13}\text{CO}$  line antenna temperature  $T_A^*$ . The offset positions from the cloud center are given at both axes in the figure. The cloud center position is  $\alpha$  (1950) =  $15^{\text{h}}51^{\text{m}}30^{\text{s}}$  and  $\delta$  (1950) =  $-4^{\circ}42'00''$ . The contour unit is in K.

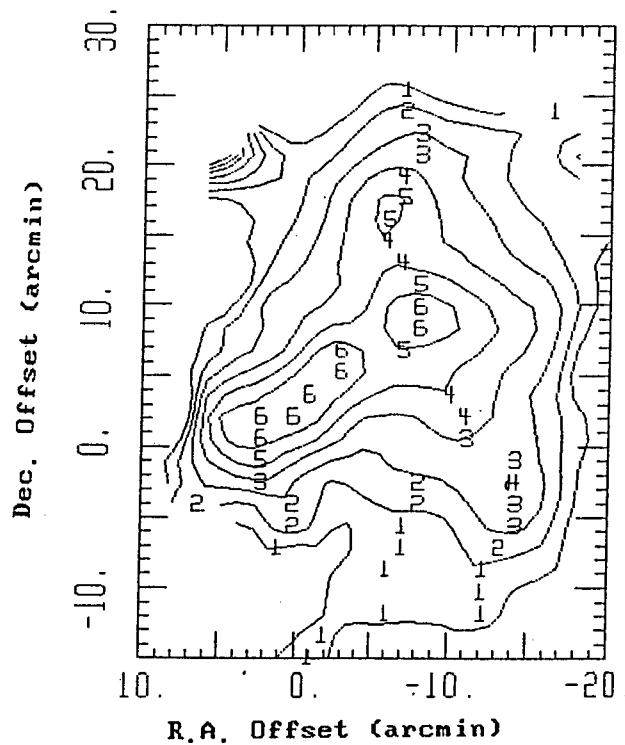


Fig. 2. Contour map of the  $^{13}\text{CO}$  integrated line intensity  $\int T_A^* dV$ . The offset positions from the cloud center are given at both axes in the figure. The contour unit is in  $\text{K km s}^{-1}$ .

per channel which corresponds to a velocity resolution of  $0.65 \text{ kms}^{-1}$  per channel. All velocities refer to the local standard of rest. The observations were corrected for the beam efficiency and for an average atmosphere attenuation using the expression for the Rayleigh-Jeans brightness temperature.

$$T_B = \frac{T_A}{\eta} \exp [ \tau \sec(z) ]$$

where  $T_A$  is the antenna temperature,  $z$  the zenith angle, and  $\tau$  is the average optical depth of the atmosphere at the zenith. We used the double position switching method. The comparison positions we used were  $0.5^\circ$  off the source position in the azimuth direction. The mapping was made by the observations with 1 arcmin spacing near the cloud center, but 2 arcmin spacing at the periphery. An integration of 3 minutes for each observing position regardless whether it is the source or the reference was performed. A total of 190 source positions have been observed. The observed line profiles are Gaussian fitted to derive the velocity and linewidth. The center position of L134 used for this mapping is  $\alpha(1950)=15^h 51^m 30^s$  and  $\delta(1950)=-4^\circ 42' 00''$ . We started the observations from the central positions moving outward until no significant signal was received. The range of the offset positions in right ascension is  $-18$  to  $7$  arcmin and  $\delta$  is  $-14$  to  $+26$  arcmin in declination.

### III. THE INTENSITY DISTRIBUTION OF $^{13}\text{CO}$

The contour map of the  $^{13}\text{CO}$  line antenna temperature  $T_A^*$  of L134 is given in Figure 1. The map shows that the maximum temperature region is extended roughly along the north-south direction, but the maximum temperature ridge is 5 to 10 arcminutes off to the right which is to the west from the cloud center. The maximum plateau is broken into two peaks, a main and a secondary, at the north of the center where the maximum  $T_A^*=5.7\text{K}$  appears. The maximum antenna temperature regions don't match the cloud center position which is about 10 arcmin east of the region. The size of the  $^{13}\text{CO}$  cloud is  $30' \times 40'$  (R.A. x Dec.) which is larger than that of the  $\text{H}_2\text{CO}$  cloud (Lee *et al.*, 1996). Figure 2 shows the contour map of the integrated line intensity,  $\int T_A^* dV$ . The peak ridge is located near the cloud center position extending toward the northwest to southeast directions diagonally, but it is broken into three components. The cloud shape is generally spherical with a size approximately 25 arcmin in right ascension and 35 arcmin in declination. The peak of integrated line intensity occurs at  $\Delta\alpha = -8'$  and  $\Delta\delta = 10'$ . The peak regions in Figures 1 and 2 don't coincide. The cloud size is approximately 25 arcmin in right ascension and 35 arcmin in declination. The  $^{13}\text{CO}$  line halfwidth distribution is given in Figure 3. It shows that the line halfwidth ranges from 0.6 to  $2.0 \text{ kms}^{-1}$ . The line halfwidth systematically increases toward the east direction. The general shape of the map is similar to that of Figure 2 with an extension along the northwest-southeast direction. This indicates that the integrated line intensity is affected mostly by the line halfwidth. The peak line halfwidth occurs at the eastern edge of the cloud which is different from the peak positions of the OH and  $\text{H}_2\text{CO}$  line halfwidths (see Mattila *et al.* 1979, Sume *et al.* 1975).

### IV. KINEMATICAL DISTRIBUTION

In Figure 4, we presented the radial velocity distribution map of the line. The range of the radial velocity is rather narrow varying from  $3.1 \text{ kms}^{-1}$  to  $2.2 \text{ kms}^{-1}$ . The velocities are comparable to those of other molecules (see Mattila *et al.* 1979, Minn 1991). The central part of the cloud show largest radial velocity and it decreases gradually to the north and south directions. This map indicates that the cloud is not rotating, but there presents a possible rolling motion. The cloud structure in the space-velocity plane is shown in Figures 5a and 5b. Figure 5a is a contour map of the integrated line intensity in the right ascension-velocity plane at 6 arcmin declination offset. Figure 5b is a contour map of the integrated line intensity in a declination-velocity plane at 0 arcmin right ascension offset. In Figure 5a, there is shown almost no velocity gradient and the structure of the cloud appears to be smooth. But in Figure 5b there presents a second small component at the velocity about  $1.0 \text{ kms}^{-1}$ , in addition to the main component at about  $3.0 \text{ kms}^{-1}$ . This component was detected earlier by Milman *et al.* (1975) at  $\alpha(1950)=15^h 51^m 29.8^s$  and  $\delta(1950)=-4^\circ 37' 31''$ . The main component has a slight velocity gradient with the declination.

## MINN AND LEE

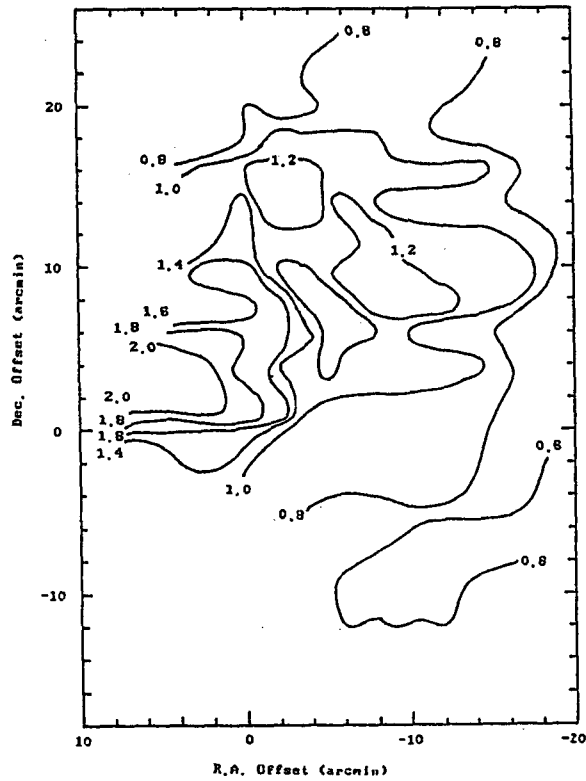


Fig. 3. Contour map of the  $^{13}\text{CO}$  line halfwidth. The offset positions from the cloud center are given at both axes in the figure. The contour unit is in  $\text{km s}^{-1}$ .

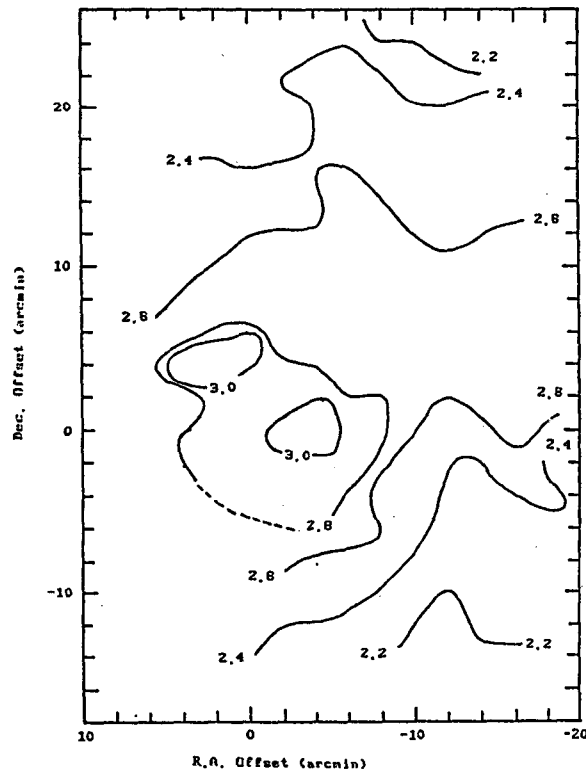


Fig. 4. Contour map of the  $^{13}\text{CO}$  line radial velocity. The offset positions from the cloud center are given at both axes in the figure. The contour unit is in  $\text{km s}^{-1}$ .

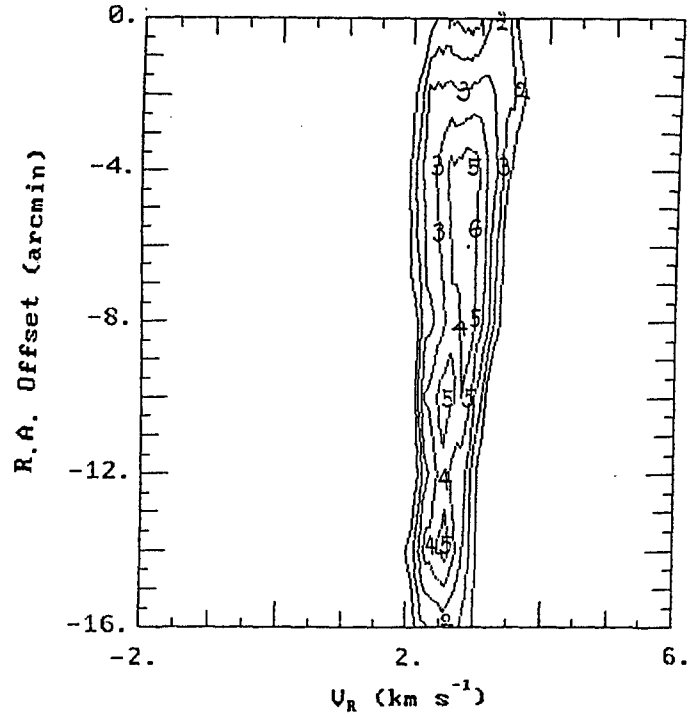


Fig. 5(a). Contour map of the  $^{13}\text{CO}$  integrated line intensity in a space-velocity plane along the declination offset  $6'$ . The ordinate shows the offset positions in right ascension from the cloud center. The contour unit is in  $\text{K km s}^{-1}$ .

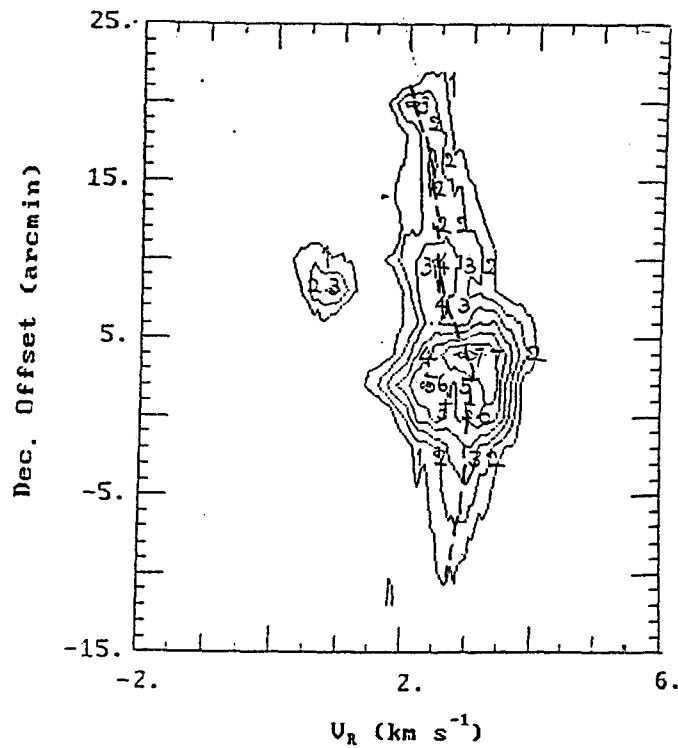


Fig. 5(b). Contour map of the  $^{13}\text{CO}$  integrated line intensity in a space-velocity plane along the right ascension offset  $0'$ . The ordinate shows the offset positions in declination from the cloud center. The contour unit is in  $\text{K km s}^{-1}$ .

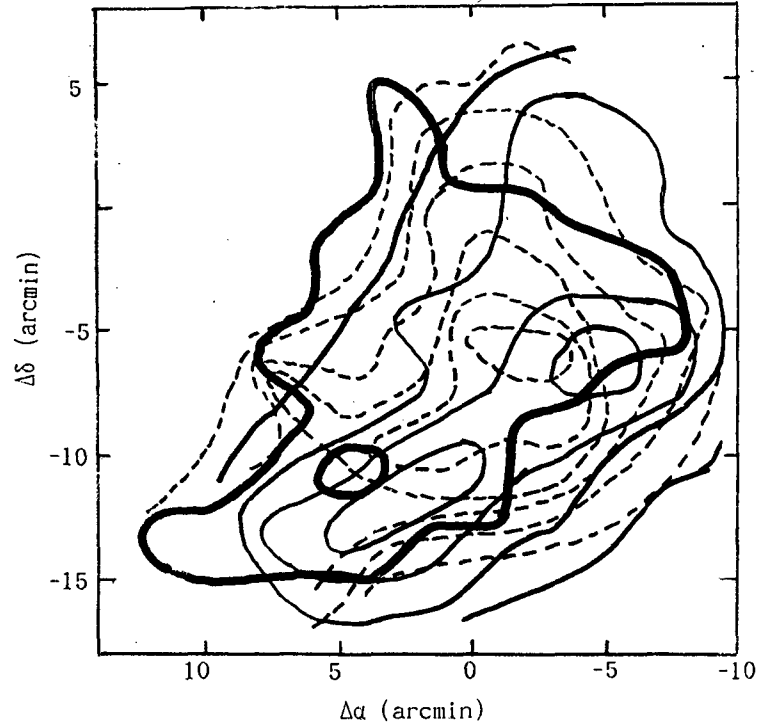


Fig. 6. Contour map of the integrated line intensities of  $^{13}\text{CO}$  (thin line) and 6-cm  $\text{H}_2\text{CO}$  (dashed line), and the visual extinction of 6.9 mag (thick line). The contour levels for  $^{13}\text{CO}$  are 1, 2, 4, 6  $\text{K kms}^{-1}$  toward the cloud center and those of  $\text{H}_2\text{CO}$  start from 0.04  $\text{K kms}^{-1}$  increasing with a 0.02  $\text{K kms}^{-1}$  interval with the maximum of 0.14  $\text{K kms}^{-1}$  at the cloud center. The cloud center is  $\alpha$  (1950) =  $15^{\text{h}}51^{\text{m}}01.0^{\text{s}}$  and  $\delta$  (1950) =  $-4^{\circ}26'51''$ .

### V. CORRELATION OF $^{13}\text{CO}$ WITH VISUAL EXTINCTION

We used the visual extinction data of this cloud derived by Cernicharo and Bachiller (1984) in order to compare with  $^{13}\text{CO}$ . They performed star counts on the prints of the Palomar Observatory Sky Survey. Their reseau size for star counts is  $2.24'$ , which is larger than the beam size of the  $^{13}\text{CO}$  observations. In order to make the reseau and beam sizes to match, we averaged the  $^{13}\text{CO}$  integrated line intensities observed at the four adjacent points. The contour lines of the observed integrated line intensities of  $^{13}\text{CO}$  and 6-cm  $\text{H}_2\text{CO}$  lines (Lee *et al.*, 1996), and the visual extinction are given in Figure 6. The map shows that the  $^{13}\text{CO}$ ,  $\text{H}_2\text{CO}$ , and dust are closely associated in space in many aspects such as the cloud shape, outer boundary, and the peak positions within the observational error. The observed integrated line intensities of  $^{13}\text{CO}$  are plotted against the visual extinction in Figure 7. Even though there are shown some scatter of points, it is apparent that there exists a linear positive correlation between the  $^{13}\text{CO}$  integrated line intensity and the visual extinction. The best fit regression line is derived as,

$$\int T_A \cdot dV(^{13}\text{CO}) = 1.3(A_V - 0.5)$$

Minn (1991) also derived a similar positive correlation between the  $\text{H}_2\text{CO}$  column density and the visual extinction in this cloud. The  $^{13}\text{CO}$  molecule line was detected at positions with visual extinction lower than about 1.0 magnitude which is much lower than those of OH and  $\text{H}_2\text{CO}$  (Mattila *et al.* 1979, Minn 1991). Laureijs *et al.* (1994) also found a tight linear correlation between  $^{13}\text{CO}$  and the blue extinction.

### VI. CONCLUSION

From the  $^{13}\text{CO}$  line mapping of L134, we conclude that this cloud has a spherical shape with an extended intensity peak ridge. The region of the cloud center has a maximum line halfwidth and the largest radial velocity. The radial

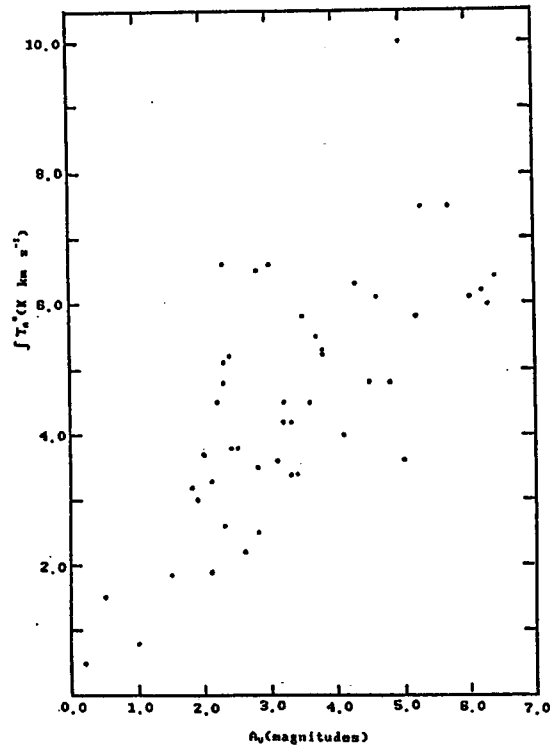


Fig. 7. The  $^{13}\text{CO}$  integrated line intensity as a function of visual extinction.

velocity decreases outward to the north and south directions from the cloud center. The line integrated intensity in the right ascension-velocity plane is smooth without much structure, but in the declination-velocity plane it shows some structure with two components. The  $^{13}\text{CO}$ ,  $\text{H}_2\text{CO}$  and visual extinction are closely correlated. The integrated line intensity of  $^{13}\text{CO}$  and visual extinction have a linear correlation.

#### ACKNOWLEDGEMENTS

We wish to acknowledge the hospitality and assistance of the staff at Taeduck Radio Astronomy Observatory. This work is supported by the grants from the Korea Astronomy Observatory and the Korea Science and Engineering Foundation.

#### REFERENCES

- Brooks, J. W., Sinclair, M. W., Manchester, G. A., & Goss, W. M. 1976, *MNRAS*, 177, 299  
 Cernicharo, J., & Bachiller, R. 1984, *A&AS*, 58, 327  
 Downes, D., Wilson, T. L., & Bieging, J., 1976, *A&A*, 52, 321  
 Laureijs, R. J., Fukui, Y., Helou, G., Mizuno, A., Imaoka, K., & Clark, F.O., 1995, *ApJS*, 101, 87  
 Lee, Y. B., Minn, Y. K., & Greenberg, J.M. 1996, in preparation  
 Mahoney, M. J., McCutcheon, W. M., & Shutter, W. L. H. 1976, *AJ*, 81, 508  
 Mattila, K., Winnberg, A., & Grasshoff, M. 1979, *A&A*, 78, 275  
 Martin, R. N., & Barrett, A. H. 1978, *ApJS*, 36, 1  
 Milman, A. S., Knapp, G. R., Knapp, S. L., & Wilson, W. J. 1975, *AJ*, 80, 101  
 Minn, Y. K. 1991, *JKAS*, 24, 191  
 Sume, A., Downes, D., & Wilson, T. L. 1975, *A&A*, 39, 435  
 Tucker, K. D., Dickman, R. L., Encrenaz, P. J., & Kutner, M. L. 1976, *ApJ*, 210, 679